PAPER • OPEN ACCESS

Design and experimental verification of a multi-pass ECRH plasma start-up scenario at a reduced magnetic field of 1.8 T at W7-X

OPEN ACCESS
IOP Publishing | International Atomic Energy Agency
Nuclear Fusion
Nucl. Fusion **66** (2026) 056017 (12pp)
https://doi.org/10.1088/1741-4326/ae5835

Design and experimental verification of a multi-pass ECRH plasma start-up scenario at a reduced magnetic field of 1.8 T at W7-X

Niklas Simon Polei[1,*], Torsten Stange[1], Kai Jakob Brunner[1], Olaf Grulke[1], Juan Fernando Guerrero Arnaiz[1], Laurent Krier[1], Heinrich Peter Laqua[1], Stefan Marsen[1], Dmitry Moseev[1], Burkhard Plaum[2], Sergiy Ponomarenko[1], Kian Rahbarnia[1], Georg Schlisio[1], Jonas Zimmermann[1] and W7X-Team[a]

[1] Max-Planck-Institute for Plasma Physics, 17491 Greifswald, Germany
[2] Institute for Interfacial Process Eng. & Plasma Technology (IGVP), University Stuttgart, 70569 Stuttgart, Germany

E-mail: niklas.simon.polei@ipp.mpg.de

Received 1 October 2025, revised 5 March 2026
Accepted for publication 27 March 2026
Published 8 April 2026

Abstract

Wendelstein 7-X (W7-X) nominally operates at a magnetic field of 2.5 T, but operation at a lower magnetic field strength is desired. The electron cyclotron resonance heating (ECRH) system of W7-X operates at 140 GHz, corresponding to second harmonic (X2) heating at 2.5 T, but also allows for heating at the third harmonic with a vacuum magnetic field around 1.7 T to 1.8 T. However, plasma start-up is not possible with X3-heating. Therefore one of the gyrotrons was tuned down to 101 GHz for an X2 breakdown of the plasma at 1.8 T on the magnetic axis. The available power in the plasma vessel for this detuned gyrotron is only 250 kW with a pulse length of the order of 50 ms. For this reason a multi-pass scenario was designed with six passes close to the magnetic axis to increase the effective power in the first few milliseconds during the breakdown. During the short 101 GHz gyrotron pulse, this X2 multi-pass scenario creates a small plasma with temperatures up to several keV and line integrated densities around 8×10^{18} m^{-2}. It could also be shown that the multi-pass scenario is necessary to achieve plasma breakdown within 50 ms. The plasma can be taken over by two sources of the neutral beam injection (NBI), starting at the same time as the detuned gyrotron to increase temperature and density. After about 1.5 s at least 3 MW of X3 ECRH are needed to take over from the NBI to maintain a stable plasma. This enables the low field operation of W7-X.

[a] See Grulke *et al* 2024 (https://doi.org/10.1088/1741-4326/ad2f4d) for the W7-X Team.
[*] Author to whom any correspondence should be addressed.

Keywords: Wendelstein 7-X, ECRH, gyrotron, plasma start-up, plasma breakdown

(Some figures may appear in colour only in the online journal)

1. Introduction

Wendelstein 7-X (W7-X) is designed to show several favorable properties of the stellarator concept on the way to a fusion power plant [1]. Among them are the good confinement properties of fast ions in high plasma-$<\beta>$ scenarios ($<\beta>$ is the ratio of kinetic and magnetic pressure). The necessary plasma-$<\beta>$ is difficult to achieve at the nominal magnetic field of 2.5 T, since around 40 MW of heating power are required. At a magnetic field of 1.8 T it is expected that only 20 MW of heating power are required to reach high plasma-$<\beta>$ values. With the foreseen upgrades of the ECRH (electron cyclotron resonance heating) system to an installed power of 18 MW [2], heating powers of this order can be reached together with the NBI (neutral beam injection) [3].

The current ECRH system of W7-X consists of eleven gyrotrons, with a maximum heating power of 8.5 MW delivered into the plasma vessel. Gyrotrons are high power microwave sources, which emit a Gaussian microwave beam with a power of the order 1 MW. At W7-X, the beams are transmitted through air via a quasi-optical multi-beam transmission line, consisting of water cooled copper mirrors, to the plasma vessel [4]. The standard heating scenarios at 2.5 T are the X2- and O2-heating, where the '2' refers to the second harmonic of the electron cyclotron frequency and X and O stand for the extraordinary and ordinary polarization of the microwave beam respectively. The X2 polarized microwave is used for plasma start-up and scenarios with densities up to $1\times 10^{20}\,\mathrm{m}^{-2}$ and has 100% absorption in the first pass through the magnetic axis. The O2 polarization is used in high density scenarios and has only about 70% absorption per pass through the magnetic axis [5].

At lower magnetic field the 140 GHz gyrotrons of the ECRH system can be used to heat the electrons at the third harmonic. Depending on the achieved plasma-$<\beta>$ values, the optimum magnetic field is between 1.7 T and 1.8 T. However, plasma start-up can not be performed with X3-heating, because a minimum temperature of 0.5 keV is needed for sufficient coupling between the electrons and the microwave [6, 7]. Plasma start-up with only the NBI is also not possible, because the interaction length is too short [8]. Instead one gyrotron can be tuned down to be resonant on the magnetic axis at 1.8 T with X2-heating. This creates a small target plasma for the NBI, for which the absorption of the NBI increases with increasing electron density [8]. Such a plasma start-up scenario with X2 and NBI at 1.8 T is developed and verified in this paper.

For that several parameters during start-up were varied, such as the prefill gas pressure or beam polarization. Similar experiments were conducted on smaller machines in preparation for the first operational campaign of W7-X. The dependence of plasma breakdown time and the neutral gas pressure were studied in Heliotron J, LHD and WEGA [9–11]. Here it was found that the plasma breakdown time shortens when the prefill gas pressure is reduced. For the microwave beam power it was found on these three machines that plasma breakdown time reduces with increasing beam power. Additionally, polarization scans were performed at CHS, Heliotron J and TJ-II [12, 13]. In these experiments it was found that the shortest breakdown time is achieved for pure X-mode polarization of the beam and increases with increasing O-mode content of the beam. The breakdown time behavior that was found in these machines with the prefill gas pressure, power and polarization is also expected to be found in W7-X in the low magnetic field scenario, since here only a small amount of ECRH energy is available for plasma start-up. At Heliotron J experiments with seed plasmas generated by non-resonant 2.45 GHz microwaves for the tangential NBI were conducted [14, 15]. There the seed plasma with a density of $10\times 10^{17}\,\mathrm{m}^{-3}$ to $10\times 10^{18}\,\mathrm{m}^{-3}$ enabled a rapid plasma start-up with the NBI.

The design of the start-up scenario for the low magnetic field is presented in section 2, in section 3 the results of plasma start-ups performed during the operational phase OP 2.2 are shown and analyzed in regard to the optimal parameters for successful start-up. Section 4 concludes this paper.

2. Start-up design

2.1. Gyrotron characteristics

All but one of the 1 MW-class gyrotrons installed at W7-X are manufactured by Thales [16], while the remaining gyrotron is a dual frequency gyrotron manufactured by CPI [17]. The transverse electromagnetic mode excited in the gyrotrons at 140 GHz are the $TE_{28,8}$ and the $TE_{28,7}$ for the Thales and CPI gyrotron respectively. The microwave is coupled out of the gyrotron through a chemical vapor deposition diamond window, which is resonant with the microwave only at specific frequencies depending on its thickness. For the windows of the W7-X gyrotrons the resonance frequency is at 140 GHz, but also at 105 GHz.

Two gyrotrons were tuned down to 101 GHz, one of the Thales gyrotrons (called C1) and the CPI gyrotron (called E5). The frequencies of the gyrotrons are 100.9 GHz and 101.25 GHz ($TE_{21,5}$ mode) for the C1 (Thales TH1507 SN001) and E5 (CPI VGT-8141A S/N 003) respectively. The important difference for the 101 GHz operation between the gyrotrons is in their internal optical elements. The launcher mirror, which converts the microwave into a Gaussian beam, is only optimized for 140 GHz in the C1 gyrotron, but in the E5 gyrotron this mirror is optimized for 140 GHz and 104 GHz. This

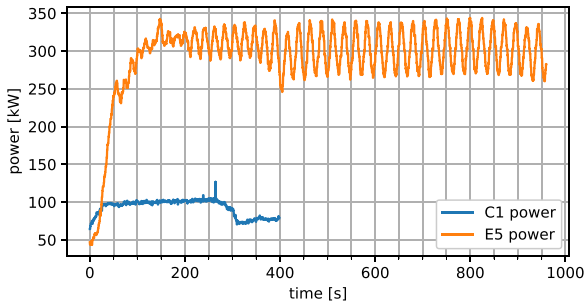

Figure 1. Averaged power output for repetitive pulsed operation of the two gyrotrons at 101 GHz measured in a calorimetric load close to the gyrotron. The pulse length and the duty cycle for the gyrotrons are as follows: C1 20 ms with 1:250, E5 50 ms with 1:300.

leads to a higher Gaussian content in the E5 beam, reducing the losses in the transmission line.

Another effect of the different launcher mirrors is in the emitted power of the gyrotron. The power output for the E5 gyrotron is 300 kW, while the C1 gyrotron emits only 100 kW (see figure 1), both measured close to the gyrotron window. The pulse length is limited to 70 ms for the E5 gyrotron, because the gas production of the spent electron beam at the collector deteriorates the vacuum. This is also the reason for the oscillating power signal, the duty cycle is 1:300, which means that 21 s are between shots, so the gas can be pumped out. The power signal has to be averaged over multiple cycles to get the emitted power. The C1 can be fired for 20 ms, after that the 101 GHz mode is lost and no power is emitted. The duty cycle for the C1 is 1:250, so there are only 5 s between shots and thus no oscillation in the power signal. The drop in the power signal after 270 s is because the gyrotron was switched off and was then restarted at 310 s. An additional limitation for the pulse length stems from the reflection of the microwave on the diamond window of the gyrotron. About 10.5% of the power of the microwave get reflected back into the gyrotron, because the frequency of 101 GHz is not exactly in the resonance of the window, which is at 105 GHz. The back-scattered microwave can heat up and damage components inside the gyrotron if the gyrotron is operated for too long. Additionally, the back-scattered microwave could be reflected back into the cavity and disturb the excited mode, leading to the loss of the excited mode [18].

It is therefore favorable to use the E5 gyrotron for low field start-up, but the C1 can be used as assistance if necessary, since the injection geometry into the plasma vessel is identical for both beamlines.

2.2. Multi-pass scenario

Due to losses in the transmission line (6%) and on the torus window (10.5%) a power of 300 kW at the gyrotron corresponds to about 250 kW delivered to the plasma vessel, which is low compared to the standard start-up scenario at 2.5 T, which uses 1 MW to 2 MW of power for plasma start-up. Additionally, the time for plasma generation is limited, due to the limited pulse length of the gyrotron, demanding an efficient initial start-up scenario. To start the ionization avalanche faster a multi-pass scenario can be employed to increase the effective power in the first few milliseconds. Multi-pass scenarios are already routinely used at W7-X for O2-heating at high densities at 2.5 T, but are limited to three passes due to the refractive nature of the plasma at high densities.

In a multi-pass scenario the beam is reflected multiple times through the plasma vessel, via the reflector tiles on the high field side wall and a polished stainless steel panel between two ECRH ports at the low field side, which are nearly parallel to each other. When a beam is injected into this poloidal plane, it can reflect multiple times nearly perpendicularly between the tiles and the panel, but it would have to be injected with a high incidence angle. However, a reflector tile with a holographic grating can reflect the beam in an arbitrary direction [19], which means that all tiles can be considered when searching for a suitable scenario, because with a holographic grating the beam can be redirected to nearly perpendicular incidence.

The raytracing code TRAVIS [20] calculates the absorption and beam path of Gaussian microwave beams in a magnetically confined plasma. It is used here to design the multi-pass scenario by comparing the absorption efficiency of different beam paths of different gyrotrons. For all gyrotrons several possible scenarios with three or more passes close to the magnetic axis were investigated. Since refraction effects can be neglected during the start-up phase, due to the low density, more than three passes through the plasma vessel can be safely realized at W7-X.

It has to be noted that TRAVIS can not take into account the ionization of neutral gas. To avoid numerical problems due to too low absorption the density and temperature were set to $7.35 \times 10^{17}\,\mathrm{m}^{-3}$ and 400 eV respectively for a comparison between the scenarios. The profiles fall off to zero at $r/a \approx 0.3$ and can be interpreted as a snapshot during a typical start-up. The calculated absorption with these parameters is about 12% per pass through the plasma, which leaves enough power for subsequent passes. The scenario which promised the highest absolute power absorption, when also considering the injected power from the respective gyrotron, was selected.

This is a scenario with six passes close to the magnetic axis for the E5/C1 beamlines, a visualization of the scenario for the C1 with TRAVIS is shown in figure 2. With this scenario the available power to start the ionization avalanche is in the range of the nominal start-up powers used at 2.5 T. For the realization of this multi-pass scenario two tiles had to be redesigned and newly manufactured. The tile which is first hit by the microwave is fitted with a holographic grating. The grating is in this case designed to reflect the beam onto a path with near perpendicular incidence on the magnetic axis after the very oblique first pass. After reflecting on the steel panel the beam hits a tile above the holographic tile. This tile also needs a modification to reflect the beam back onto the magnetic axis and on a good position on the steel panel to allow for two further passes. In this case slanting the surface by 1.9° in the poloidal direction and 0.6° in the toroidal direction is enough to redirect the beam onto the magnetic axis. The surface of the

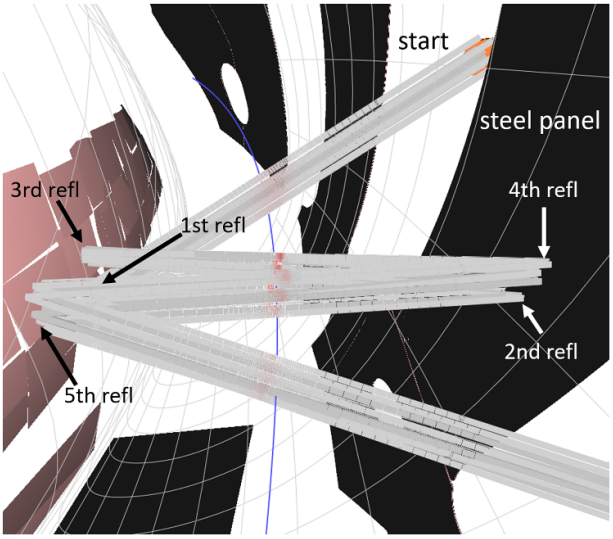

Figure 2. Multi-pass scenario designed with the raytracing code TRAVIS. Six passes are close to the magnetic axis. Two new tiles have to be designed and manufactured.

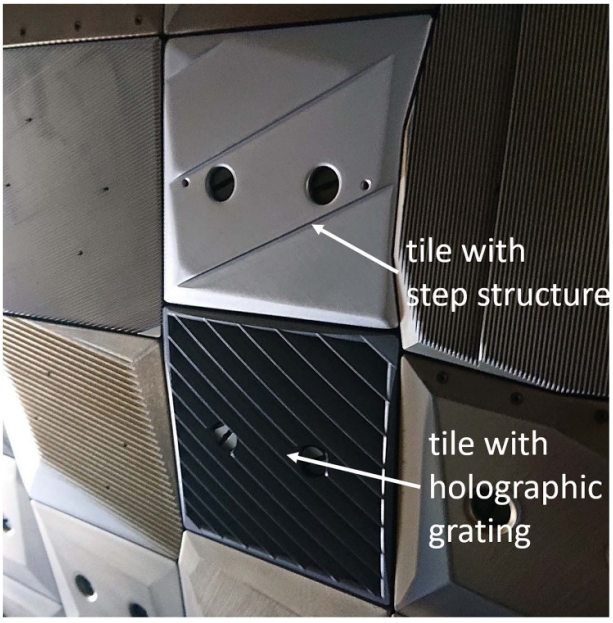

Figure 3. The two new tiles for the multi-pass scenario installed for the C1 beam line. The black tile is the holographic tile manufactured from graphite. The whitish tile is the tile with the step structure manufactured from graphite, coated with tungsten.

tile is equipped with a step structure in order to create no leading edges, with the step height being half the wavelength to mitigate interference losses. The tiles installed in the machine can be seen in figure 3, where the black tile is the holographic tile and the whitish one above, the tile with the step structure.

The oblique angle in the first pass, causes a high mode conversion rate in the first reflection of 18.7%, subsequent reflections have significantly less mode conversion (below 1% for the 2nd and 3rd reflection and 10% for the 4th reflection), so the back conversion from O- to X-mode is small. The power

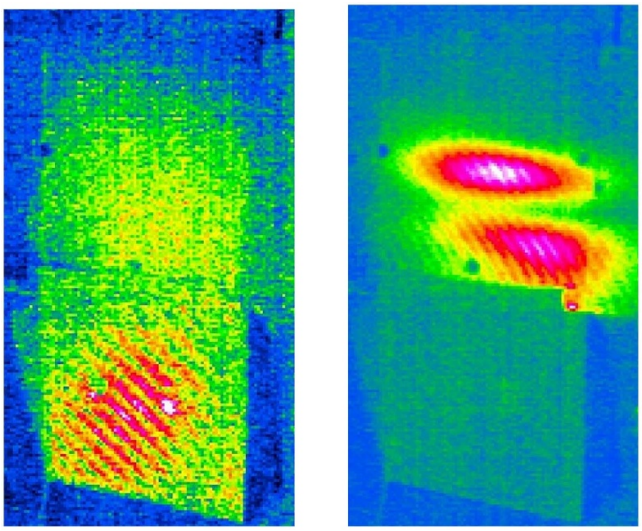

Figure 4. Microwave beam on the holographic tile (left image) and tile with step structure (right image) for the C1 beamline. The relevant spot on the right image is the top one, the lower beam spot is another reflection of the panel, which is caused by the orientation of the PVC target. On both tiles the beam is slightly below center, but was corrected accordingly, so the beam moves to the center.

that is converted to O2-mode will not get absorbed and therefore can not contribute to plasma start-up. So the polarization should be adjusted to 100% X2-mode in the second pass. This way the O2-mode content after the six passes is 30% lower than for the case with 100% X2-mode polarization in the first pass.

The beam path was verified in the plasma vessel by observing PVC targets, placed on the tiles and steel panel, with an IR camera. The PVC targets heat up when hit by the microwave. The optimal position of the steerable plasma facing mirror inside the plasma vessel could also be found in these measurements. When the beam is pointed at the middle of the holographic tile it hits the tile with the step structure in the middle as well, as designed. The corresponding IR images are shown in figure 4. Additionally the calculated beam radii for all passes at the location of the magnetic axis are shown in table 1. The focal point of the beam that is injected into the plasma vessel lies 70 mm after the reflection at the steel panel. After the focal point it diverges again, but in poloidal direction it gets refocused with every reflection at the steel panel, because the steel panel has a curvature radius of 1435 mm in poloidal direction. In the toroidal direction the steel panel is flat (this can also be seen in figure 2).

3. Start-up results

3.1. Prediction of start-up parameters

Looking at past start-ups with comparatively low power at W7-X (see figure 5), the achievable plasma parameters can be predicted. There were nine successful start-ups with 400 kW of power and one successful start-up with 600 kW.

Table 1. The beam radii at the location of the magnetic axis for each pass.

Pass	Pol. radius (mm)	Tor. radius (mm)
1	49.3	49.3
2	37.3	37.3
3	18.9	35.7
4	39.9	45.3
5	49.6	60.8
6	31.0	78.2

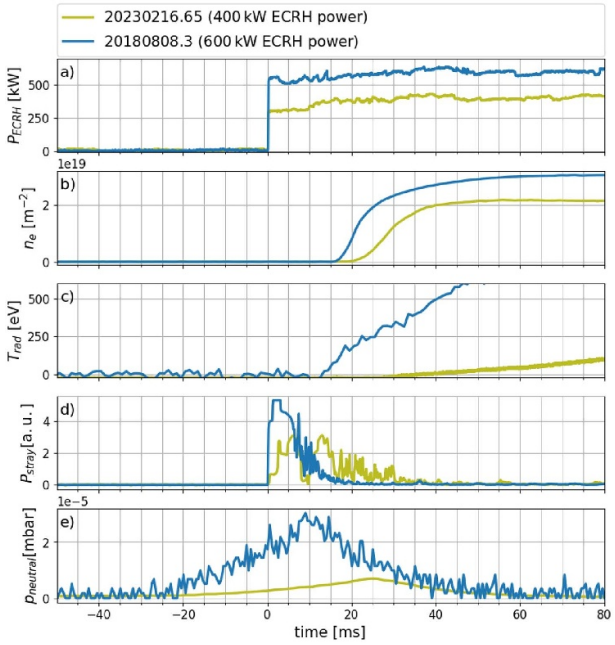

Figure 5. Start-ups with low power from previous campaigns with 600 kW and 400 kW. Panel (*a*) shows the ECRH power, panel (*b*) the line integrated density and panel (*c*) the electron temperature. In panel (*d*) the data from the sniffer probes are shown and panel (*e*) shows the neutral gas pressure.

In program 20180808.3 600 kW of ECRH power with one pass through the resonance layer in the plasma center, a second pass crossed the resonance layer at $r/a \approx 0.4$, and a hydrogen prefill of 50 ms from one valve is used for plasma start-up, the resulting neutral gas pressure measured by the neutral pressure gauges, which are hot cathode ionization gauges [21], can be seen in panel '(*e*)' of figure 5. However, the neutral gas pressure is subject to an error of up to a factor of two. To evaluate the density evolution during plasma start-up, post-processed data from the integral-electron density dispersion interferometer (IEDDI) were used [22]. Most of the programs were evaluated using a recently developed neural network based evaluation scheme with a high bandwidth, 20 μs time delay and a systematic error of roughly 5×10^{17} m^{-2} [23]. The electron temperature is measured by the ECE (electron cyclotron emission) system [24] and is usually underestimated at these plasma parameters, because the plasma is not optically thick. The measured radiation temperature T_{rad} is in general lower than the real electron temperature T_e. The optical thickness increases with electron density and temperature. For an electron density of $n_e = 2 \times 10^{19}$m^{-3} and electron temperature T_e of 0.15 keV to 0.4 keV, a ratio of radiation temperature to electron temperature of about $T_{\mathrm{rad}} = 0.66 \cdot T_e$ to $T_{\mathrm{rad}} = 0.95 \cdot T_e$ is expected. The density and temperature start to rise after 12 ms (panel '(*b*)' and '(*c*)' in figure 5). The density reaches 3×10^{19} m^{-2} after another 30 ms, at that point $T_{\mathrm{rad}} = 0.55$ keV.

One of the programs with 400 kW for plasma start-up is used as an example (program 20 230 216.65). Here the beam passed twice through the resonance layer. In this program a hydrogen prefill of 25 ms from two valves is used. The density and temperature rise after 20 ms (panel '(*b*)' and '(*c*)' in figure 5), the density reaches 2×10^{19} m^{-2} after another 25 ms, where $T_{\mathrm{rad}} = 0.1$ keV. Additionally in panel '(*d*)' of figure 5 the sniffer probe signal is shown, measuring the stray radiation [25]. The sniffer probe supports the measurements of the ECE and the interferometer and also suggests a longer plasma start-up time for the 400 kW example than for the 600 kW program.

From this it can be inferred that without a multi-pass the E5 would take longer than 20 ms to establish a plasma. However, with the multi-pass scenario, it should take less than 10 ms, which is the typical start-up time for 1 MW to 2 MW.

Additionally, a first estimation of the plasma parameters with a heating power of 250 kW can be done by simple downscaling of the presented program examples. For that both programs were analyzed with TRAVIS using the experimental data as input to TRAVIS. The temperature and density were updated in 1 ms steps and the deposition profile of the ECRH was calculated for each time step. This was done until 250 kW of power were absorbed. This will give an estimation of the plasma parameters which can be reached with the 250 kW 101 GHz beam at 1.8 T.

In program 20 180 808.3 after 17 ms 250 kW of the beam power are absorbed and the plasma parameters at this time point are $\int n dl = 1.1 \times 10^{19}$m^{-2}, $T_{\mathrm{rad}} = 0.2$ keV. In program 20 230 216.65 after 48 ms 250 kW of the microwave are absorbed with $\int n dl = 2.1 \times 10^{19}$m^{-2} and $T_{\mathrm{rad}} = 0.12$ keV. The underestimation of the temperature gives a lower limit of the electron temperature.

From this data a plasma with a density above 1×10^{19} m^{-2} with a temperature below 0.2 keV is expected. This is not sufficient for direct X3 take-over. Instead the plasma first has to be taken over by the NBI to increase density and temperature before the X3 can take over. An NBI take-over with two sources should be possible, one source might suffice. This can be inferred from previous work by Gradic *et al* [8], where it is shown that, for 1.7 MW of NBI power, a pre-ionization of the neutral gas can reduce the NBI plasma start-up time significantly, if the density is high enough ($n_e > 10^{17}$ m^{-3}).

3.2. *Initial start-up phase with ECRH only*

Important diagnostics for the analysis of the start-up attempts are the IEDDI measuring the line integrated density, which can be used for quantitative comparisons between the scenarios, but cannot be used exclusively for the success of take-over attempts analyzed later in the paper. The core electron temperature measured by the newly commissioned W-band

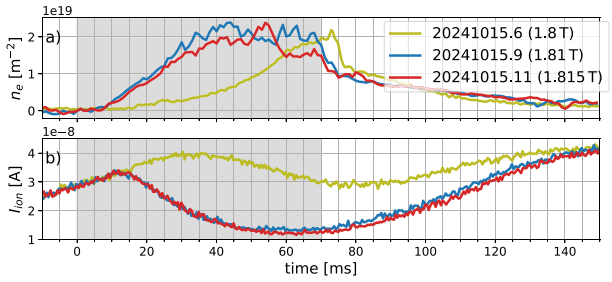

Figure 6. Results of the magnetic field scan programs, the ECRH was running from 0 ms to 70 ms, the gas prefill was 15 ms. (*a*) shows the line integrated density, for program 20 241 015.6 the real-time data is shown[3] and (*b*) shows the neutral gas pressure. For these programs no temperature measurements are available.

ECE radiometer, an upgrade to the ECE diagnostic at W7-X to measure the second harmonic ECE at low magnetic field operation, can be only be used as a lower limit of the actual electron temperature, since most of the plasmas without NBI are optically thin. The diamagnetic loops [26] are measuring the diamagnetic energy. They are an important tool to assess the success of NBI take-over, but the sensitivity is limited. Finally, the stray radiation measurements by the sniffer probe are an important tool to assess ECRH absorption. The sniffer probe used in the following experiments measures the stray radiation at 101 GHz and was installed specifically for the observation of plasma start-up experiments, because the 140 GHz sniffer probes are too insensitive at 101 GHz.

In a series of start-up attempts the magnetic field strength on-axis, neutral gas pressure, ECRH power, polarization of the beam and aiming position of the beam were varied, to find the optimal conditions for plasma start-up.

For the magnetic field scan (shown in figure 6) the E5 was operated for 70 ms and the C1 for 20 ms, both starting at $t = 0$ ms. Magnetic field strengths on the magnetic axis of 1.80 T, 1.81 T and 1.815 T were tested. The optimal magnetic field strength is around 1.81 T to 1.815 T. In the experiment the difference in the achieved line integrated density (measured by the IEDDI), between the field strengths of 1.81 T and 1.815 T, is in the order of 10% (panel '(*a*)' in figure 6). The density rises from the zero-level after 11 ms to densities above 2×10^{19} m^{-2} within 30 ms for both programs, while for the program performed at 1.80 T the rise from zero-level starts after 15 ms and it takes an additional 55 ms to reach 2×10^{19} m^{-2}. As an additional quantity to assess start-up performance the neutral gas pressure can be used as a proxy for the ionization rate. Since there was no calibration of the neutral gas pressure gauges performed for helium at the reduced field, the measured ion current is given, which is proportional to the neutral gas pressure. Even though the neutral gas pressure for

[3] For this program only the real-time density data was available, which has a significant systematic differential error for this measurement regime. In addition the real-time data is automatically filtered with a strong low-pass filter with a time constant of roughly 7.5 ms, explaining the 15 ms time delay with respect to the unfiltered data. Nonetheless the real-time data qualitatively agrees with the unfiltered data.

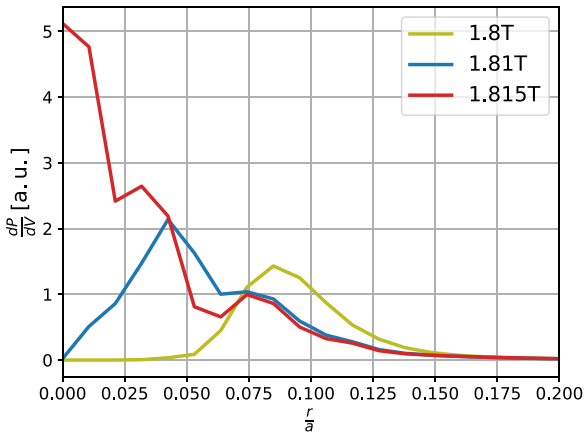

Figure 7. Power density of the 101 GHz microwave beam for different magnetic fields.

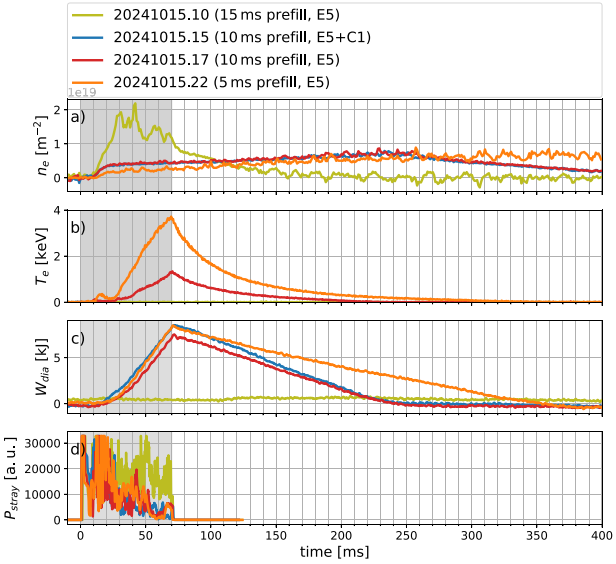

Figure 8. Results of the helium prefill scan, the ECRH was running from 0 ms to 70 ms. (*a*) shows the density, (*b*) shows the temperature measured by the W-band ECE system, which was only available for the shorter prefill durations. Panel (*c*) displays the diamagnetic energy, panel (*d*) the sniffer signal.

1.815 T is only slightly smaller than for 1.81 T (panel '(*b*)' in figure 6), the rest of the parameter optimization was conducted at 1.815 T, if not otherwise specified. The increase of the neutral gas pressure after the switch off of the gyrotron is due to recombination. The difference in start-up performance stems most likely from the different resonance positions of the 101 GHz microwave at the different magnetic fields and therefore different power deposition (see figure 7). The maximum of the power deposition for 1.815 T, 1.81 T and 1.80 T is at $\frac{r}{a} = 0$, $\frac{r}{a} = 0.042$ and $\frac{r}{a} = 0.085$ respectively. For the volume of a torus the minor radius enters squared, so when moving from 1.81 T to 1.80 T, the volume, that is heated by the same amount of heating power, quadruples.

The neutral gas pressure was varied by varying the length of the helium prefill (see figure 8), with only the E5 active for 70 ms. The prefill durations were 15 ms, 10 ms and 5 ms.

Experiments with longer prefill duration were conducted as well, but with even longer prefills worse results were achieved, as will be seen in section 3.3 NBI take-over phase. The gas prefill of all experiments presented in this paper starts 95 ms before the program start. For a prefill duration of 15 ms no complete plasma breakdown was achieved. Although the density rises to more than $2 \times 10^{19}\,\mathrm{m}^{-2}$ (panel '(*a*)' in figure 8), the diamagnetic energy stays at its noise level (panel '(*c*)' in figure 8). The plasma is only generated in a small tube around the magnetic axis and decays exponentially after heating shut-off. Electron temperature data is not available here. For the other two prefill durations, a plasma, which fills out the complete plasma vessel of W7-X (visible in the video camera diagnostic), could be formed. The densities reach around $8 \times 10^{18}\,\mathrm{m}^{-2}$. The core electron temperature measured by the W-band ECE is about 1.35 keV for the 10 ms prefill and reaches up to 3.8 keV for the 5 ms prefill (panel '(*b*)' in figure 8). The measured temperature is close to the actual electron temperature for the 10 ms and 5 ms cases, since the sniffer is close to zero, which means the plasma is optically thick for the microwave. The temperature is higher for the shorter prefill, because the same power of the microwave beam is transferred to a smaller number of electrons. The significantly higher temperature leads to a higher diamagnetic energy for the shorter prefill of 5 ms. It should be noted that the diamagnetic energy can have an error of up to 2 kJ. In this case however, the slightly higher diamagnetic energy for the 5 ms prefill is plausible, since the densities are comparable, but the temperature is higher by nearly a factor of 2.8 in the plasma center. This ratio decreases towards 1 when moving away from the plasma center, which explains why the diamagnetic energies are still comparable. The higher temperatures for the shorter prefills of 10 ms and 5 ms are most likely also the reason for the delayed collapse of the plasma, because the higher temperatures are preventing recombination. Whereas for the 15 ms prefill case the temperature is close to zero when the gyrotron is switched off and the recombination process starts immediately. The further expansion of the hot plasma up to the last closed flux surface in the 10 ms and 5 ms cases leads to further ionization and an increase in the line integrated density. The sniffer signal (panel '(*d*)' in figure 8) shows that the stray radiation goes down for both programs, although it does not reach zero completely, the absorption is close to 100%. This is further supported by TRAVIS calculations, which suggest that more than 98% of the microwave is absorbed in the first pass in both cases at the end of the gyrotron pulse for the present plasma conditions.

A program with 10 ms prefill (identical to 20 241 015.17) was performed with the C1 firing as well between 0 ms and 20 ms (see 20 241 015.15). The density that was reached is the same as without the C1, but the diamagnetic energy is higher, which suggests that the temperature was higher as well, but lower than for program 20 241 015.22. However, a temperature measurement was not available for this program. The difference in diamagnetic energy between the two programs 20 241 015.17 and 20 241 015.15 is within the errors, but a higher electron temperature is plausible, because the density is the same but the injected energy by the ECRH is higher.

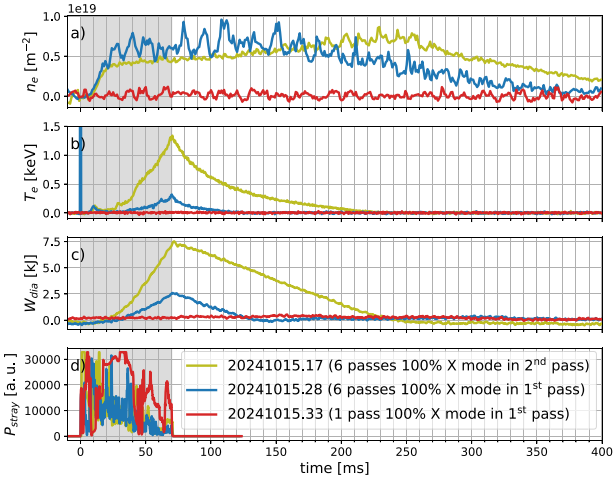

Figure 9. Results of the change of polarization and mirror settings, the ECRH was running from 0 ms to 70 ms. (*a*) shows the density, in panel (*b*) the electron temperature measured by the W-band ECE system can be seen, in panel (*c*) the diamagnetic energy is presented, panel (*d*) shows the sniffer signal.

Since the temperature reached by the E5 alone is more than sufficient for the NBI take-over and the C1 is more efficiently used for the later X3-take-over at 140 GHz, for the rest of the experiments only the E5 was used, as well as a helium prefill of 10 ms, if not otherwise specified.

The results of the variation of polarization and mirror position are shown in figure 9. The program 20 241 015.17 is used as a reference for the optimum that was found so far. In the program 20 241 015.28 the polarization was switched to 100% X2-mode in the first pass. Although plasma breakdown is also achieved here and the density is comparable (panel '(*a*)' in figure 9), the temperature is lower at about 0.33 keV in its maximum (panel '(*b*)' in figure 9). The sniffer for these two programs is at a low level, which means that the plasma is optically thick and the measured temperatures are close to the actual electron temperature. In program 20 241 015.33 the mirrors were set to perpendicular incidence (only one pass through the vessel), as in the standard X2 start-up scenario at 2.5 T, and the polarization was set to 100% X2-mode in the first pass. No plasma was created, density and diamagnetic energy stay at zero and the stray radiation is at a high level and does not get less over time, which can be seen in the signal of the sniffer probe (panel '(*d*)' in figure 9). That means that there is only very little absorption in this case.

Taking a closer look at the neutral gas pressure during the program 20 241 015.33 with only one pass through the magnetic axis, there is ionization happening. A small dip in the neutral gas pressure (panel '(*a*)' in figure 10) at the end of the ECRH pulse suggests that the power of 250 kW is enough to ionize neutral gas. However, with only one pass through the plasma the absorbed power is lower than for the multi-pass. The losses by recombination and plasma expansion are then making up a higher fraction of the absorbed power, which prolongs the onset time of the ionization avalanche. With a longer ECRH pulse the ionization avalanche should be triggered, but a longer ECRH pulse is not possible with the pulse length limitation of the detuned gyrotrons.

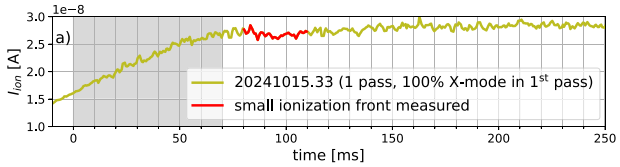

Figure 10. A closer look at the program 20 241 015.33 with only one pass through the magnetic axis, shows that there is only very little ionization, as can be seen in the neutral gas pressure in panel (*a*).

Additionally one can estimate the energy gain of an electron at the very start of the ionization phase with the equation derived by Farina [27]

$$W_{\max} \cong 2.1 \cdot \frac{P^{1/2}}{fw\left(1 - N_{||}^2\right)^{1/2}} \tag{1}$$

where $W_{\max}$ is the energy gain, P the microwave power, f the microwave frequency, w the beam width and $N_{||}$ the parallel refractive index. Inserting the values of the experiment ($P = 0.25\,\mathrm{MW}, f = 101.25\,\mathrm{GHz}, w = 0.098\,\mathrm{m}$ and $N_{||} = 0$) one obtains a maximum energy gain of 105.82 eV, this is much larger than the ionization energy of 24.6 eV of Helium.

Therefore the multi-pass scenario needs to be employed, so that the effective power available in the first few milliseconds is increased, to start the ionization avalanche faster. When additionally the polarization is adjusted for 100% X2-mode in the second pass the electron temperature is four times higher than for a 100% X2-mode polarized beam in the first pass.

In OP 2.2 (at the end of 2024) start-up was performed only in helium. However, in OP 2.3 (at the beginning of 2025) the prefill gas type was changed to hydrogen and plasma start-up also worked good. Unfortunately no identical programs were run in helium and hydrogen, so no direct comparison between the two can be made, but figure 11 shows a comparison of plasma start-ups in helium and in hydrogen. The differences between the two programs, except for the working gas, are that the E5 gyrotron was operated for 70 ms in the 2024 program and for 50 ms in the 2025 program, additionally the magnetic field strength is different, 1.815 T in 2024 and 1.80 T in 2025. For both prefill gases the plasma fills out the whole plasma volume (visible in the video cameras). The density (panel '(*b*)' in figure 11) shows similar behavior for both prefill gases as well, with the ionization avalanche starting after 10 ms. The stray radiation signal (panel '(*c*)' of figure 11) indicates for both programs that nearly all of the gyrotron power is absorbed towards the end of the pulse, because the stray radiation goes down to zero at a similar speed. Start-up is therefore possible in both gases giving flexibility in the scenario.

3.3. NBI take-over phase

NBI take-over attempts were performed on several experiment days with different NBI timing, gas prefill durations and NBI power.

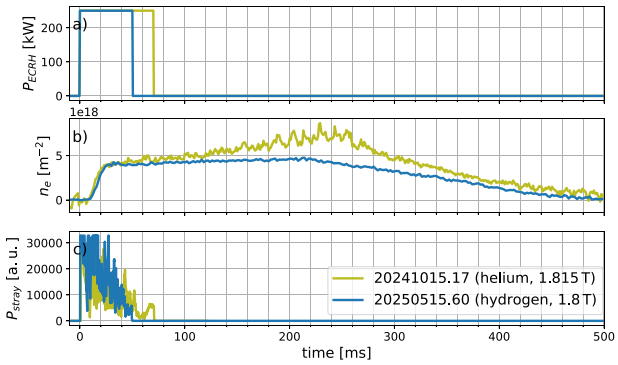

Figure 11. Comparison of start-ups in helium and hydrogen. In panel (*a*) the ECRH power is displayed. Panel (*b*) shows the line integrated density and panel (*c*) the stray radiation.

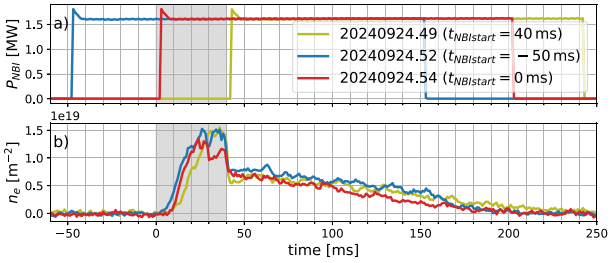

Figure 12. Results of the NBI timing experiments, the ECRH was running from 0 ms to 40 ms and the gas prefill was 40 ms. Panel (*a*) shows the NBI pulse and panel (*b*) the density.

In the foreseen scenario, the NBI starts at the end of the ECRH pulse. However, in the experiment this timing showed the worst results. For all three programs a suboptimal gas prefill of 40 ms and a magnetic field of 1.80 T was used, this is because these experiments were performed before the optimal values were determined. In figure 12 three different timings of the NBI are shown, at the end of the ECRH, NBI starting 50 ms before the ECRH and simultaneous start with the ECRH. To find the best timing the smallest relative drop in density (panel '(*b*)' in figure 12), after the ECRH is switched off, is desired. For that the density at 39 ms is compared to the density at 42 ms. The highest ratio between the densities is reached for the simultaneous start of ECRH and NBI, the density after the switch-off is 66% of that before the switch-off. The largest relative drop in density is observed when the NBI is switched on at the end of the ECRH pulse, here the density is only 42% of that before the switch-off of the gyrotron. For the NBI start before the ECRH switch-on, the ratio is 54%. Therefore from here on, the timing of the NBI was set to a simultaneous start with the ECRH.

The provided NBI power is also an important parameter. One NBI source is not enough for the take-over of the plasma, this can be seen in figure 13, where for both programs a gas prefill of 10 ms was used. Here in the program where only one NBI source fired, the program was aborted due to a too low diamagnetic energy (panel '(*d*)' in figure 13). The density (panel '(*b*)' in figure 13) rises only very slowly while the temperature (panel '(*c*)' in figure 13), measured by Thomson

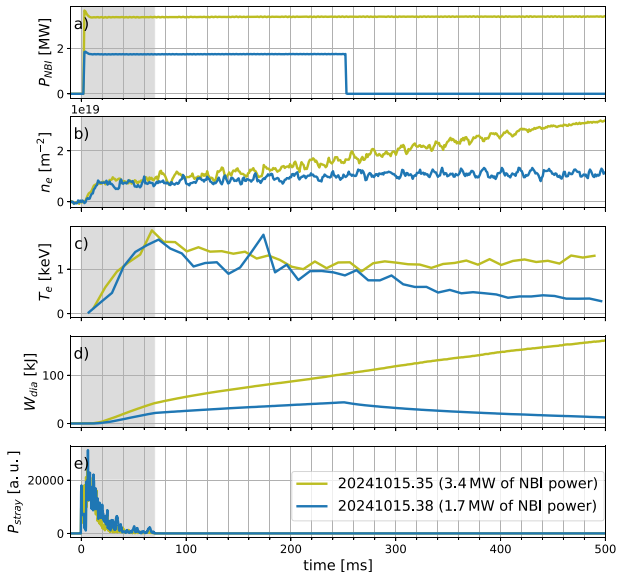

Figure 13. Results with different NBI power, the ECRH was running from 0 ms to 70 ms and the gas prefill was 10 ms. (*a*) shows the NBI power. In panel (*b*) the density is displayed. The temperature measured by Thomson scattering is shown in panel (*c*), the diamagnetic energy is shown in panel (*d*), in panel (*e*) the sniffer signal is displayed.

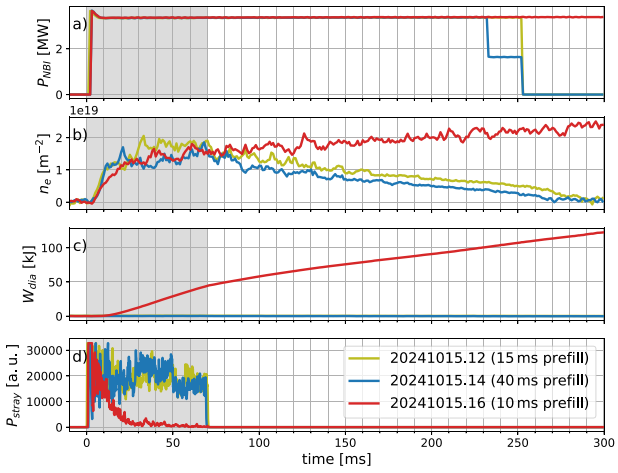

Figure 14. Results of the gas prefill variation for the NBI take-over, the ECRH was running from 0 ms to 70 ms. Panel (*a*) shows the NBI power. In panel (*b*) the density is presented, the diamagnetic energy is shown in panel (*c*), in panel (*d*) the sniffer signal is displayed.

scattering [28], decreases after the ECRH is switched off at 70 ms. This initially also happens when using two NBI sources, but the density increases at a faster rate and the temperature recovers and starts to rise as well after 350 ms to 400 ms. This increases the diamagnetic energy, so the take-over is successful and does not get aborted by a safety interlock. This is suspected to be due to the number of fast ions generated by the NBI, which are twice as many for two sources. Since there is nearly 100% shine through of the NBI beam at these low densities [29], the number of fast ions generated by the small absorbed fraction of power is important. For both programs the sniffer signal does decrease to zero (panel '(*e*)' in figure 13), which means that in both cases close to 100% absorption of the ECRH is achieved, which was cross-checked with TRAVIS calculations for the plasma conditions in these cases yielding theoretically more than 99% absorption for the first pass, so the successful take-over is determined by the NBI power.

The results of the gas prefill duration, which plays a significant role in the NBI take-over as well, can be seen in figure 14. The NBI can not sustain the plasma, if the gas prefill is too long. This is most likely due to a lower electron temperature of the plasma created by the E5 gyrotron. A prefill duration of 15 ms, 40 ms and 10 ms was tested. ECRH and NBI get switched on simultaneously at 0 ms and the density (panel '(*b*)' in figure 14) starts to rise at the same time as well. The densities reached are also of the same order. However, when the ECRH gets switched off at 70 ms, the NBI can only sustain the plasma with the 10 ms prefill. For the other two programs the density slowly decreases after the ECRH switch-off, but does not fall to zero as fast as for ECRH only (compare to panel '(*a*)' in figure 6). Although no temperature measurement is available for these programs, one can infer from the diamagnetic energy (panel '(*c*)' in figure 14) that the temperature was low, because the diamagnetic energy does not rise above the zero level. But the temperature seems to be the important parameter for the success of the take-over here, because the densities are the same for the start-up phase, where the ECRH is running as well. That the electron temperature plays a significant role was shown in an earlier work by Gradic *et al* [8], because the reaction rate increases by five orders of magnitude when going from a few eV to 100 eV, after that the reaction rate drops again but only by one order of magnitude. Finally one can infer from the sniffer signal (shown in panel '(*d*)' of figure 14) that for the longer prefill durations of 15 ms and 40 ms the ECRH absorption is poor, because the stray radiation level does not go down, compared to the successful NBI take-over, with 10 ms prefill, where the stray radiation reduces to zero within 30 ms.

In conclusion the NBI ideally starts at the same time as the ECRH and two NBI sources are needed for a successful take-over. The optimal gas prefill for the successful take-over is a prefill of 10 ms, the same as for ECRH only, where a prefill of 10 ms also performed very good (compare to figure 8) and was only outperformed by a prefill of 5 ms, which was not tested together with the NBI.

3.4. X3 take-over phase

Finally, the NBI plasma has to be taken over by the X3 ECRH. The timing of the X3 ECRH, as well as the ECRH power were varied (the results are presented in figure 15). In program 20 240 925.36 the X3 ECRH was switched on at the end of the NBI pulse and in programs 20 241 015.23 and 20 241 015.35 there is an overlap of 150 ms between X3 ECRH and NBI. The short increase in NBI power in program 20 241 015.23 is due to a third source blipping for charge exchange recombination spectroscopy. The ECRH power was varied between

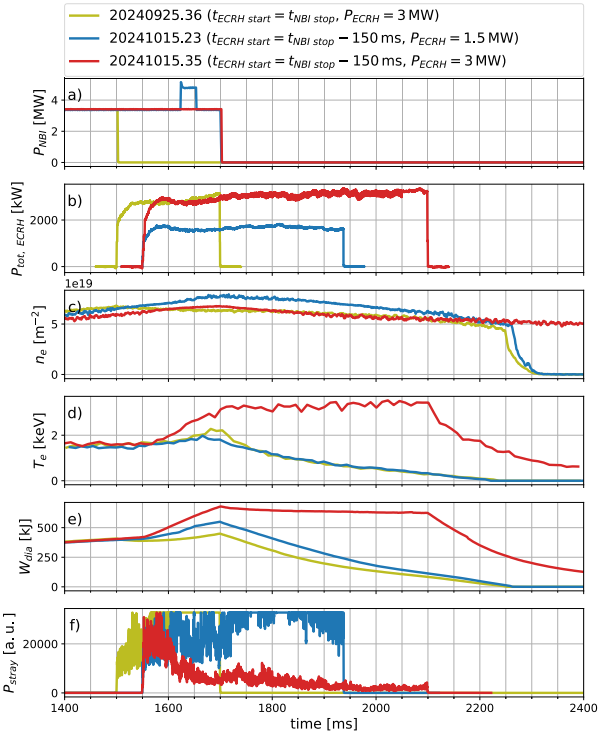

Figure 15. Results of the X3 take-over. Panel (*a*) shows the NBI power, panel (*b*) shows the ECRH power and panel (*c*) the density. The temperature measured by Thomson scattering is displayed in panel (*d*), the diamagnetic energy in panel (*e*) and in panel (*f*) the sniffer signal is shown.

3 MW and 1.5 MW. When switching on the X3 ECRH (panel '(*b*)' in figure 15) after the NBI pulse (panel '(*a*)' in figure 15), the ECRH can not take over the plasma. The same applies for only 1.5 MW of power with an overlap between ECRH and NBI. The density (panel '(*c*)' in figure 15) goes down, after the NBI is switched off, for all three programs, this is to be expected, because the particle fuelling stops. For all three programs the temperature (panel '(*d*)' in figure 15) rises slowly in the beginning of the ECRH pulse. But only for 3 MW of ECRH overlapping with the NBI, the temperature as well as the diamagnetic energy show a drastic increase almost immediately with ECRH start and the stray radiation measured by the sniffer reduces significantly. The sniffer signal can be seen in panel '(*f*)' of figure 15. It does not go down for the other two programs. For the 3 MW ECRH, which is switched on 150 ms before the end of the NBI pulse, the sniffer signal does decrease to a low level after about 100 ms and stays close to zero even in the ECRH only phase. Here the temperature increases significantly and the diamagnetic energy (panel '(*e*)' in figure 15) is constant at a high level. From this point on the X3 ECRH pulse can be prolonged to at least several seconds with stable plasma parameters when the density feedback is used.

3.5. The role of the machine condition

Typically, at the beginning of each experiment session at W7-X, wall cleaning discharges are run, which consist of a large

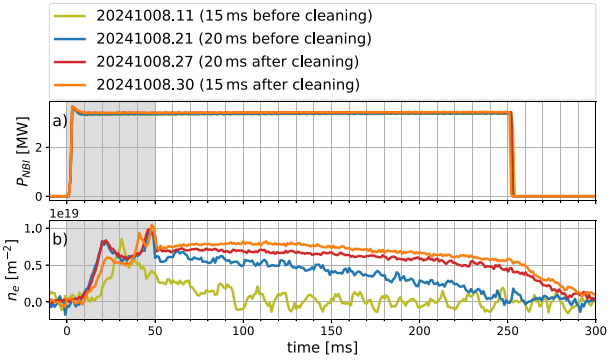

Figure 16. Several programs with similar settings to demonstrate the impact of ECRH cleaning of the machine, the ECRH was running from 0 ms to 50 ms. Panel (*a*) shows the NBI power and panel (*b*) displays the density.

number of 100 ms ECRH pulses. This is not possible at the reduced field of 1.8 T because of the non-absorption of the X3 ECRH when there is no plasma present. Before the experiment session with the first start-up experiments on 24 and 25 September 2024 there were pulse trains run. But before the experiment session on 8 October 2024 there were no cleaning discharges run. This had a strong impact on start-up success (see figure 16). This can be seen in the densities in panel '(*b*)' of figure 16. The first program of the session with NBI had a much lower density (factor 2) than expected from the session before and the plasma was gone before the NBI switched off. This was the fastest density decay seen in any low-field start-up program. Over time, just by continuing plasma start-up attempts, the machine was cleaned gradually. The density rises earlier after 12 ms and a plasma can be maintained for 150 ms longer. After that the magnetic field of the machine was ramped up to 2.5 T, two ECRH cleaning pulse trains were run and the magnetic field reduced back to 1.8 T. After that two programs with identical settings as the programs before the cleaning were run. The difference in start-up performance is clearly visible. The density can be maintained longer and at a higher level.

Before the experiment session on 15 October 2024, again two ECRH cleaning pulse trains were run and the start-up attempts in that session were successful, when using the same settings as on 8 October 2024. The available ECRH power at 101 GHz, in addition to the maximum pulse length of the E5 gyrotron, makes good machine conditions necessary for successful start-up.

4. Conclusion

A plasma start-up scenario with minimal ECRH power for the low magnetic field operation of W7-X at 1.8 T was designed and verified. For that two gyrotrons were tuned down to 101 GHz, with one of those having a power output of 300 kW, of which 250 kW are delivered into the plasma vessel. A multi-pass scenario with six passes close to the magnetic axis was designed, utilizing two modified first-wall reflection tiles. One of those tiles is fitted with a holographic grating, reflecting the beam in the desired direction. The surface of the second tile is

slanted slightly and equipped with a step structure, redirecting the beam onto the magnetic axis. The multi-pass scenario was then verified with PVC targets and an IR camera in the plasma vessel during the maintenance phase.

In the experimental campaign OP 2.2, the start-up scenario was experimentally verified and careful optimizations of magnetic field, gas prefill, beam polarization as well as the timing and power of NBI and X3 ECRH were performed. In programs with only the start-up gyrotron the optimal parameters for an initial start-up with ECRH were found to be a magnetic field strength on the axis of 1.81 T to 1.815 T, a gas prefill of 5 ms to 10 ms and a polarization of 100% X2-mode in the second pass. With these parameters an electron temperature of several keV and a density above $5 \times 10^{18}\,\mathrm{m}^{-2}$ were reached. This is a much higher temperature than predicted beforehand (up to a factor of 10), but the densities are lower, which is caused by a shorter gas prefill. The gas type of the prefill can be helium or hydrogen. Plasma start-up works in both gases.

The NBI take-over is successful when X2 ECRH and NBI start simultaneously and at least two NBI sources are used. The NBI is usually operated for 1.5 s to allow the plasma to expand into the whole plasma vessel and to increase the density to $7.5 \times 10^{19}\,\mathrm{m}^{-2}$ and the temperature to 1.5 keV.

The NBI plasma can be taken over by the X3 ECRH when the X3 is switched on 100 ms to 150 ms before the NBI pulse ends. An ECRH power of at least 3 MW is necessary, because a lower power does not increase the plasma-$<\beta>$ fast enough. At the end of a 450 ms X3 only phase the central electron temperature is at 4 keV and the density at $5 \times 10^{19}\,\mathrm{m}^{-2}$, because no density feedback was used. The sniffer signal goes down close to zero, which means that the X3 phase can be prolonged to several seconds.

An important parameter for the success of plasma start-up is the machine condition. If the machine walls are potentially contaminated with impurities, the plasma build-up cannot be sustained and start-up fails. ECRH cleaning pulse trains are therefore necessary before the 1.80 T operation.

The plasma start-up scenario developed here was routinely used in several sessions of low magnetic field operation in OP 2.3 at the beginning of 2025. During the experimental campaign the start-up scenario was optimized further. The magnetic field was changed to 1.80 T, to move the X3 heating resonance closer to the magnetic axis, and the X3 take-over from the NBI was performed after already 1 s of NBI operation. The prefill gas was changed to hydrogen with no degradation in performance. Different magnetic field configurations were run, without problems in the start-up phase.

The numerical values presented here for the important parameters for plasma start-up, such as the gas prefill length or heating timings, are specific to the situation at W7-X. However, the methodology of the scenario design and optimization of parameters for successful plasma start-up can be transferred to other machines. Furthermore, the multi-pass scenario could be adapted in general for low ECRH power plasma start-ups, as it was shown that multiple passes reduce the time for the onset of the ionization avalanche.

Acknowledgments

This work has been carried out within the framework of the EUROfusion Consortium, funded by the European Union via the Euratom Research and Training Programme (Grant Agreement No. 101052200 - EUROfusion). Views and opinions expressed are however those of the author(s) only and do not necessarily reflect those of the European Union or the European Commission. Neither the European Union nor the European Commission can be held responsible for them.

ORCID iDs

Torsten Stange 0000-0003-4154-1455
Kai Jakob Brunner 0000-0002-0974-0457
Juan Fernando Guerrero Arnaiz 0000-0002-7650-2918
Laurent Krier 0000-0003-0627-1074
Kian Rahbarnia 0000-0002-5550-1801
Georg Schlisio 0000-0002-5430-0645

References

[1] Erckmann V. *et al* 1997 The W7-X project: scientific basis and technical realization *17th IEEE/NPSS Symp. Fusion Engineering (Cat. No. 97 CH36131)* vol 1 (IEEE) pp 40–48
[2] Laqua H.P. *et al* 2023 The ECRH-power upgrade at the Wendelstein 7-X stellarator *EPJ Web Conf.* **277** 04003
[3] Lazerson S.A. *et al* 2021 First neutral beam experiments on Wendelstein 7-X *Nucl. Fusion* **61** 096008
[4] Stange T. *et al* 2017 Advanced electron cyclotron heating and current drive experiments on the stellarator Wendelstein 7-X *EPJ Web Conf.* **157** 02008
[5] Laqua H.P. *et al* 2006 The steady-state ECRH-system at Wendelstein 7-X *Proc. 15th Int. Stellarator Workshop Tech. Meeting Innobatuve Concepts Theory Stellarator* (*Madrid, Spain, 10–11 October 2005*) pp 856–9
[6] Marushchenko N.B. *et al* 2019 Reduced field Scenario with X3 heating in W7-X *EPJ Web Conf.* **203** 01006
[7] Johansson C.A. and Aleynikov P. 2024 Electron cyclotron resonance during plasma initiation *J. Plasma Phys.* **90** 905900103
[8] Gradic D., Dinklage A., Brakel R., McNeely P., Osakabe M., Rust N. and Wolf R. 2015 Assessment of the plasma start-up in Wendelstein 7-X with neutral beam injection *Nucl. Fusion* **55** 033002
[9] Cappa A., Castejón F., Tabarés F.L. and Tafalla D. 2001 Second harmonic electron cyclotron plasma breakdown in TJ-II *Nucl. Fusion* **41** 363
[10] Preynas M. *et al* 2014 Study of plasma start-up initiated by second harmonic electron cyclotron resonance heating on WEGA experiment *AIP Conf. Proc.* **1580** 498–501
[11] Preynas M. *et al* 2015 Experimental characterization of plasma start-up using ECRH in preparation of W7-X operation *EPJ Web Conf.* **87** 02005
[12] Nagasaki K. *et al* 2004 Experimental study of plasma breakdown by second harmonic electron cyclotron waves in Heliotron J *Nucl. Fusion* **45** 13
[13] Nagasaki K. *et al* 2006 Plasma breakdown using second-harmonic EC waves in helical devices *JOURNAL-Korean Phys. Soc.* **49** S18

[14] Kobayashi S. *et al* 2011 Plasma startup using neutral beam injection assisted by 2.45 GHz microwaves in Heliotron J *Nucl. Fusion* **51** 062002
[15] Kobayashi S. *et al* 2020 Study of seed plasma generation for NBI plasma start-up using non-resonant microwave launch in Heliotron J *Plasma Phys. Control Fusion* **62** 065009
[16] Albertia S. *et al* 2001 European high-power CW gyrotron development for ECRH systems *Fusion Eng. Des.* **53** 387–97
[17] Cauffman S. *et al* 2016 Design and testing of a dual-frequency 104/140 GHz megawatt-class gyrotron for fusion plasma heating *2016 IEEE Int. Conf. on Plasma Science (ICOPS)* (*Banff, Alberta, Canada*, *19–23 June 2016*) (IEEE) pp 1–1
[18] Antonsen T.M., Cai S.Y. and Nusinovich G.S. 1992 Effect of window reflection on gyrotron operation *Phys. Fluids B* **4** 4131–9
[19] Plaum B. *et al* 2019 Development of reflection gratings for advanced ECRH scenarios *EPJ Web Conf.* **203** 04012
[20] Marushchenko N.B., Turkin Y. and Maassberg H. 2014 Ray-tracing code TRAVIS for ECR heating, EC current drive and ECE diagnostic *Comput. Phys. Commun.* **185** 165–76
[21] Wenzel U. *et al* 2019 Performance of new crystal cathode pressure gauges for long-pulse operation in the Wendelstein 7-X stellarator *Rev. Sci. Instrum.* **90** 2019
[22] Brunner K.J. *et al* 2018 Real-time dispersion interferometry for density feedback in fusion devices *J. Instrum.* **13** 09002
[23] Brunner K.J. Fuchert G., de Amorim Resende F.B.L., Knauer J., Hirsch M. and Wolf R.C. 2025 Auto-encoding quadrature components of modulated dispersion interferometers *Plasma Phys. Control Fusion* **67** 105007
[24] Hirsch M. *et al* 2019 ECE diagnostic for the initial operation of Wendelstein 7-X *EPJ Web Conf.* **203** 03007
[25] Moseev D., Laqua H.P., Marsen S., Stange T., Braune H., Erckmann V., Gellert F. and Oosterbeek J.W. 2016 Absolute calibration of sniffer probes on Wendelstein 7-X *Rev. Sci. Instrum.* **87** 083505
[26] Rahbarnia K. *et al* 2018 Diamagnetic energy measurement during the first operational phase at the Wendelstein 7-X stellarator *Nucl. Fusion* **58** 096010
[27] Farina D. 2018 Nonlinear collisionless electron cyclotron interaction in the pre-ionisation stage *Nucl. Fusion* **58** 066012
[28] Pasch E., Beurskens M.N.A., Bozhenkov S.A., Fuchert G., Knauer J. and Wolf R.C. 2016 The Thomson scattering system at Wendelstein 7-X *Rev. Sci. Instrum.* **87** 11E729
[29] Rust N., Heinemann B., Mendelevitch B., Peacock A. and Smirnow M. 2011 W7-X neutral-beam-injection: selection of the NBI source positions for experiment start-up *Fusion Eng. Des.* **86** 728–31